Food Chemistry 170 (2015) 360–365

Contents lists available at ScienceDirect

Food Chemistry

journal homepage: www.elsevier.com/locate/foodchem

Analytical Methods

Sensitive determination of carbendazim in orange juice by electrode modified with hybrid material

Claudia A. Razzino [a], Lívia F. Sgobbi [a], Thiago C. Canevari [a,*], Juliana Cancino [b], Sergio A.S. Machado [a]

[a] Instituto de Química de São Carlos, Universidade de São Paulo, PO Box 780, 13560-970 São Carlos, SP, Brazil
[b] Instituto de Física de São Carlos, Universidade de São Paulo, PO Box 780, 13560-970 São Carlos, SP, Brazil

ARTICLE INFO

Article history:
Received 17 December 2013
Received in revised form 5 August 2014
Accepted 6 August 2014
Available online 27 August 2014

Keywords:
Pesticides
Carbendazim
Mesoporous silica
Carbon nanotubes
Electrochemical sensor

ABSTRACT

This paper describes the application of a glassy carbon electrode modified with a thin film of mesoporous silica/multiwalled carbon nanotubes for voltammetric determination of the fungicide carbendazim (CBZ). The hybrid material, (SiO_2/MWCNT), was obtained by a sol–gel process using HF as the catalyst. The amperometric response to CBZ was measured at +0.73 V *vs.* Ag/AgCl by square wave voltammetry at pH 8.0. SiO_2/MWCNT/GCE responded to CBZ in the linear range from 0.2 to 4.0 μmol L^{-1}. The calculated detection limit was 0.056 μmol L^{-1}, obtained using statistical methods. The SiO_2/MWCNT/GCE sensor presented as the main characteristics high sensitivity, low detection limit and robustness, allowing CBZ determination in untreated real samples. In addition, this strategy afforded remarkable selectivity for CBZ against ascorbic and citric acid which are the main compounds of the orange juice. The excellent sensitivity and selectivity yielded feasible application for CBZ detection in orange juice sample.

© 2014 Elsevier Ltd. All rights reserved.

1. Introduction

Carbendazim (CBZ, methyl 2-benzimidazolecarbamate) is a benzimidazole fungicide widely used to control citrus black spot (a fungal disease) in Brazil, Mexico and Costa Rica, which are the top three source of orange juice imported into the USA (Buch, Brown, Niva, Sautter, & Sousa, 2013). The European Union has established maximum residue limits (MRLs) for carbendazim in citrus ranging between 100 and 700 ppb (0.52 and 3.6 μmol L^{-1}) (Risk Assessment for Safety of Orange Juice Containing Fungicide Carbendazim, 2012). The Environmental Protection Agency (EPA) allowed limited use of CBZ in citrus fruit until 2009. Currently, the use of CBZ is not approved in the USA (Risk Assessment for Safety of Orange Juice Containing Fungicide Carbendazim, 2012). Due to the high consumption of orange juice in the world and the high environmental impact that may result, the control of CBZ levels is extremely important. Several analytical methods are used for CBZ detection such as high-performance liquid chromatography (Subhani, Huang, Zhu, & Zhu, 2013; Wen et al., 2013), mass spectroscopy (Domínguez-Álvarez, Mateos-Vivas, García-Gómez, Rodríguez-Gonzalo, & Carabias-Martínez, 2013; Gilbert-López, García-Reyes, & Molina-Díaz, 2012), UV–Vis and fluorescence spectroscopies (del Pozo, Hernández, & Quintana, 2010; Llorent-Martínez, Fernández-de Córdova, Ruiz-Medina, & Ortega-Barrales, 2012). However, these techniques are not suitable for *in situ* and real-time detection, besides they require complex pre-treatment steps, highly trained operators and time-consuming detection processes. To overcome these drawbacks, electroanalytical techniques have been applied. A variety of modified electrodes have been used to determine trace amounts of CBZ in different matrix, but not in orange juice (Guo, Guo, Li, Wang, & Dong, 2011; Hernandez, Ballesteros, Galan, & Hernandez, 1996; Luo, Wu, & Gou, 2013; Manisankar, Selvanathan, & Vedhi, 2005).

Inorganic–organic hybrid material based on mesoporous silica obtained by the sol–gel process have been employed in different areas (Backe, Day, & Field, 2013; Ewlad-Ahmed, Morris, Patwardhan, & Gibson, 2012; Qu, Alvarez, & Li, 2012), including the electroanalytical field (Walcarius, 2013; Walcarius, Mandler, Cox, Collinson, & Lev, 2005). These hybrid materials have the advantage of combining distinct organic and inorganic components, giving rise to a composite with new properties. The properties of the inorganic–organic hybrid material include high porosity with pore diameters ranging between 2 and 50 nm, which facilitates the process of mass transfer, as well as high chemical stability and stiffness (Hasanzadeh, Shadjou, Eskandani, & de la Guardia, 2012). The main organic compound used in the synthesis of these hybrid materials is carbon nanotubes (MWCNT). These composites have been the subject of intense research in electrochemical sensing, owing to their intrinsic structural, electronic and chemical

* Corresponding author. Tel./fax: +55 16 3521 3109.
E-mail address: tccanevari@gmail.com (T.C. Canevari).

http://dx.doi.org/10.1016/j.foodchem.2014.08.085
0308-8146/© 2014 Elsevier Ltd. All rights reserved.

properties, such as large specific surface, high conductivity, good biocompatibility, and so on (Yang et al., 2010).

We have recently demonstrated the electrochemistry of mesoporous inorganic–organic hybrid material onto glassy carbon electrodes and its application to the electrocatalytic oxidation of dopamine, uric acid and paracetamol in urine (Canevari, Raymundo-Pereira, Landers, Benvenutti, & Machado, 2013). Herein, we proposed the application of the hybrid material to determine CBZ levels in orange juice. The modified electrode has good sensitivity, rapid response time, reproducibility, remarkable stability and low detection limit (LOD). The application of the modified electrode towards the quantification of CBZ in orange juice samples was found to be promising.

2. Methodology

2.1. Reagents

Tetraethyl orthosilicate (TEOS, 98%), multiwall carbon nanotubes (MWCNT, diameter: 110–170 nm, 99.9%), carbendazim (CBZ, 97%) and Nafion solution 117 were purchased from Sigma–Aldrich and hydrofluoric acid (HF, 48%) was purchased from Synth. Phosphate buffer solution (0.1 mol L^{-1}) was prepared from NaH_2PO_4 and Na_2HPO_4 (Sigma–Aldrich PA reagents). All aqueous solutions were prepared with ultrapure water obtained from a Milli-Q Plus system (Millipore).

2.2. Synthesis of mesoporous inorganic–organic hybrid material

Inorganic–organic hybrid material (mesoporous silica containing carbon nanotubes, SiO_2/MWCNT) was synthesized following the procedure described by Canevari, Raymundo-Pereira, Landers, Benvenutti, and Machado (2013) with some modifications. The hybrid material obtained was not submitted to acid treatment for carbon nanotubes functionalization providing different properties to this material. Initially, a TEOS solution was prepared by dissolving 0.045 mol in an equal volume of ethanol under stirring for 20 min. Then, 4 mL of H_2O were added, maintaining the proportion of Si/H_2O (1:4) and 0.9 g of MWCNT was added to the mixture. The suspension was ultrasonicated for 20 min. To the resulting mixture, 0.3 mL of HF was added under sonication until gel formation. The obtained gel was stored for up to 7 days at room temperature. Then, the xerogel was ground and the powder was washed with ethanol in a Soxhlet extractor for 2 h and submitted to a heat treatment at 323 K to evaporate all residual solvent. The resulting material was designated as SiO_2/MWCNT.

2.3. Electrode modification

The glassy carbon electrode (GCE, Φ = 5 mm) was polished with 1.0, 0.3 and 0.05 μm alumina slurries, and then ultrasonicated in ethanol and water for 5 min. Prior to surface modification, the GCE was electrochemically conditioned by repetitive cyclic voltammetry (CV) in H_2SO_4 0.1 mol L^{-1} in a potential range from 0 to 1 V. For thin film deposition, 25 mg of the SiO_2/MWCNT solid were mixed in 5 mL H_2O and 10 μL of a 5% Nafion solution, and ultrasonicated for 10 min. Then, 15 μL of SiO_2/MWCNT suspension were cast onto the GCE surface and dried at room temperature. After that, the electrode was immersed in 0.1 mol L^{-1} phosphate buffer pH 8.0 for 1 h to hydrate the film layer. The modified electrode was designated as SiO_2/MWCNT/GCE.

3. Instrumentation

The Brunauer–Emmett–Teller (BET) method was employed to calculate the specific surface areas (S_{BET}) and the BJH method was employed to study the pore distribution of the hybrid material, SiO_2/MWCNT. Adsorption–desorption isotherms were measured at 77 K on a Micromeritics TriStar II Krypton instrument model (Georgia, USA). The samples were previously outgassed at 400 K for 10 h.

X-ray photoelectron spectroscopy (XPS) of SiO_2/MWCNT was carried out on a VSW HA 100 hemispherical electron analyzer model (Scientific Instrument Ltda, Manchester, UK), using an Al anode as the X-ray source. The X-ray source was operated at 12 keV and 15 mA. The correction of the binding energies for charge was obtained using the reference Si2p line from silica, which was set at 103.4 eV.

The morphologies of SiO_2/MWCNT were analysed by field emission gun scanning electron microscopy (FEG-SEM) using a FEG-Zeiss model Supra 35VP (Zeiss, Germany) equipped with a high-resolution secondary electron detector (in-lens detector) operating at 6.0 kV and a point-to-point resolution of 3.8 nm.

High-resolution transmission electron microscopy (HR-TEM) images were obtained in a FEI TECNAI G^2 F20 model (FEI Philips, Netherlands) microscope operating at 200 kV. The powder samples were ultrasonically suspended in ethanol for 30 min, and the suspension was dropped onto carbon-coated copper grids.

Electrochemical measurements were performed on a model PGSTAT 302 Autolab electrochemical system (Eco Chemie, Netherlands) controlled by the NOVA software (Eco Chemie, Netherlands) using a conventional electrochemical cell with a working electrode (SiO_2/MWCNT/GCE), reference electrode (Ag/AgCl) and counter electrode (Pt), at room temperature.

4. Results and discussion

4.1. Structural characterization

SiO_2/MWCNT hybrid material exhibited type IV isotherms with type H2 hysteresis, characteristic of a disordered mesoporous material with a heterogeneous pore distribution (Lowell, Shields, Thomas, & Thommes, 2004; Sing et al., 1985) with average pore size of 13 nm (Supplementary data). SiO_2/MWCNT presented a surface area (S_{BET}) and pore volume (P_V) of 386 m^2 g^{-1} and 0.82 cm^3 g^{-1}, respectively. The high pore volume confirmed the mesoporosity of the hybrid material which facilitated the mass transfer rate of the analyte in the porous structure of the material. This characteristic is relevant for electrochemical sensor development enhancing its sensitivity.

4.2. X-ray photoelectron spectroscopy (XPS)

The XPS spectra and binding energy values of the C1s and O1s core levels are shown in Fig. 1A and B. The C1s XPS spectrum clearly indicated five components corresponding to carbon atoms with different functional groups: C—C (284.75 eV), C—OH (286.4 eV), C=O (288.7 eV), O—C=O (291.1 eV) and (292.75 eV) (Chiang, Lin, & Chang, 2011; Kundu, Wang, Xia, & Muhler, 2008; Zhou et al., 2007). It is important to highlight that acid treatment was not carried out on SiO_2/MWCNT. Therefore, we suggest that these functional groups can be related to the MWCNT production process or by the effect of oxygen present in the atmosphere that can generate functional groups. The O1s spectrum showed two components of the binding energy; the value of 532.9 eV was attributed to the O of O—Si and the binding energy of 530.6 eV was assigned to oxygen bonded to carbon atoms, suggesting the presence of functional groups (Canevari, Vinhas, Landers, & Gushikem, 2011; Chiang et al., 2011).

The Si2p spectrum of the SiO_2/MWCNT material presented an intense peak with a binding energy of 103.3 eV (data not shown), indicating the formation of silica (Canevari et al., 2011).

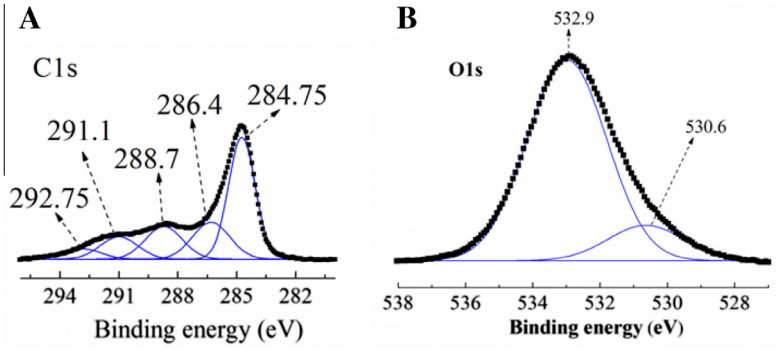

Fig. 1. XPS spectra of the SiO_2/MWCNT hybrid material: binding energy values of C1s and O1s core levels.

4.3. SEM images and HR-TEM micrographs

The field emission gun scanning electron microscopy (FEG-SEM) image of SiO_2/MWCNT showed that MWCNT were well-dispersed in the framework silica with variable lengths and diameters (Fig. 2A). The SEM image shows that MWCNT were physically incorporated into the silica matrix. The physical incorporation of MWCNT occurred because CNTs were not previously submitted to acid treatment and therefore, they did not participate in the formation of mesoporous silica network. This proposal was confirmed through high magnification HR-TEM micrograph of MWCNT embedded within the mesoporous silica matrix (Fig. 2B).

4.4. Electrochemical behaviour of CBZ at the modified electrode

The difference in the electrochemical behaviour of CBZ at GCE, MWCNT/GCE and SiO_2/MWCNT/GCE were evaluated by square wave voltammetry in 0.1 mol L^{-1} phosphate buffer pH 8.0, containing 2.0 μmol L^{-1} CBZ, at scan rate of 20 mV s^{-1} (Fig. 3). No peak related to the carbendazim oxidation was observed for the bare glassy carbon electrode which indicates GCE does not exhibit electrocatalytic activity for carbendazim. In contrast, when the determination was performed at the MWCNT/GCE and SiO_2/MWCNT/GCE electrodes, there was a peak for carbendazim at 0.713 and 0.688 V, respectively. These peaks indicate that both MWCNT/GCE and SiO_2/MWCNT/GCE electrodes exhibit electrocatalytic activity and can identify the fungicide carbendazim. However, the electrode modified with the hybrid material, SiO_2/MWCNT/GCE, showed a better electrocatalytic response (higher catalytic current and the potential was less positive) compared to the electrode modified only with MWCNT. It can be explained due to the carbon nanotubes physically incorporated into the mesoporous silica matrix were oriented in such a way that their

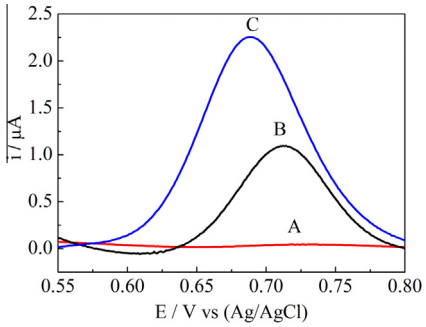

Fig. 3. SWV of (A) bare GCE, (B) MWCNT/GCE and (C) SiO_2/MWCNT/GCE in 0.1 mol L^{-1} phosphate buffer pH 8.0 containing 2.0 μmol L^{-1} CBZ.

extremities were more susceptible to reacting with the fungicide carbendazim, as shown in the HR-TEM images. To determine the best electrocatalytic response of the hybrid material, SiO_2/MWCNT/GCE, in relation to the carbon nanotubes, MWCNT/GCE, electrochemical impedance spectroscopy was performed under open circuit conditions, in 0.1 mol L^{-1} phosphate buffer pH 8.0, containing 3.0 mmol L^{-1} $[Fe(CN)_6]^{3-}$/$[Fe(CN)_6]^{4-}$ (Supplementary data). The semicircle in the Nyquist plot is attributed to the capacitive resistance owing to the charge transfer resistance (Rct) in the oxidation of Fe^{2+}/Fe^{3+} at the electrode–solution interface. As it can be seen, the Rct values were significantly different, i.e. 13.37 kΩ for SiO_2/MWCNT/GCE, 21.48 kΩ for MWCNT/GCE and 17.33 kΩ for GCE. Therefore, the lower value of Rct presented by the hybrid material SiO_2/MWCNT/GCE can be associated with faster reaction kinetics, generating enhanced electrocatalytic response, consistent with the square wave voltammetry results.

The effects of the scan rate (v) on the peak current of CBZ at SiO_2/MWCNT/GCE were investigated by cyclic voltammetry in

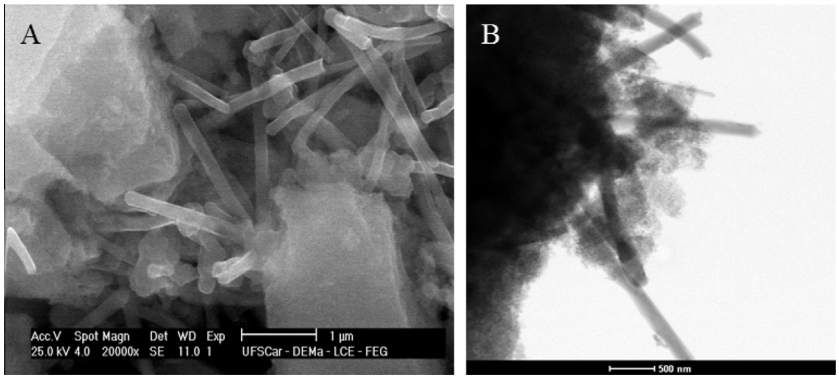

Fig. 2. (A) FEG-SEM image of SiO_2/MWCNT. Magnification: 20,000×. (B) HR-TEM micrograph of SiO_2/MWCNT hybrid material at high magnification.

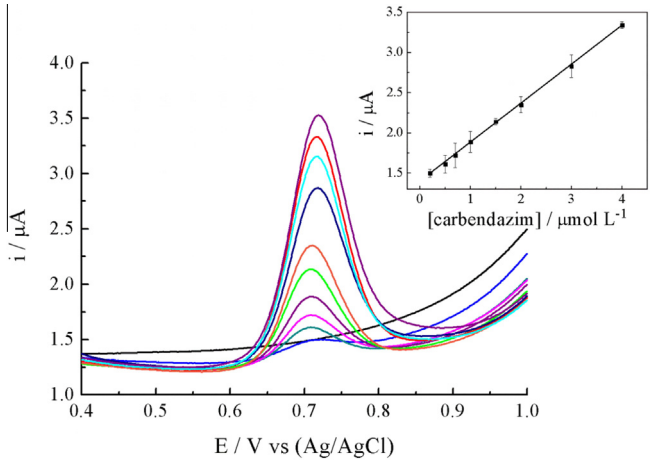

Fig. 4. A SWV of SiO_2/MWCNT/GCE with CBZ concentrations ranging from 0.2 to 4.0 µmol L^{-1}, in 0.1 mol L^{-1} phosphate buffer pH 8.0. Inset: Calibration curve of peak current *vs.* CBZ concentration.

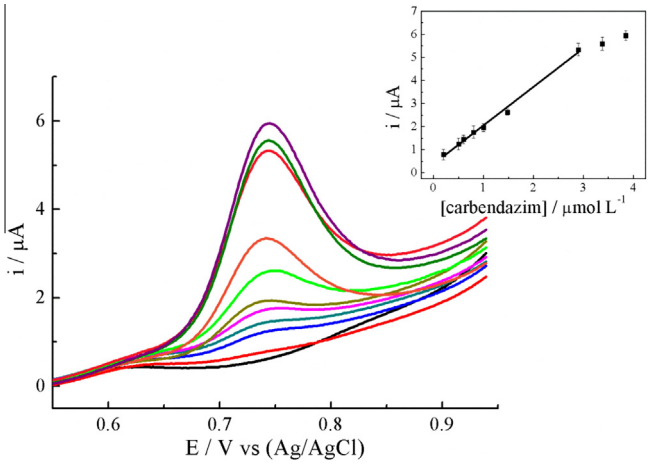

Fig. 5. SWV for the addition of different amounts of CBZ (0.2, 0.5, 0.6, 0.8, 1.0, 1.5 and 3.0 µmol L^{-1}) in a real sample solution. Inset: Plot of peak current *vs.* added CBZ concentration.

the range from 10 to 300 mV s^{-1}. The anodic peak current (i_{pa}) increased linearly with the square root of the scan rate, confirming a diffusion-controlled process with a linear correlation coefficient of $r = 0.9973$, according to i_{pa} (A) = $1.40 \times 10^{-7} + 3.79 \times 10^{-6}$ $v^{1/2}$ (V s^{-1})$^{1/2}$ (Supplementary data).

The effect of pH on the electrooxidation potential (E) of CBZ was performed in 0.1 mol L^{-1} phosphate buffer with the pH range of 3.0–8.0, keeping the concentration of carbendazim fixed at 2.0 µmol L^{-1}. It was also noted that the anodic peak potential (E) shifted to less positive potentials with an increase in the pH value. These shift in the potential (E) is due to the oxidation carbendazim process involving protons and electrons. Despite the greater current intensity in pH 5.0, the pH chosen for the present analysis was pH 8.0 ($E = 0.72$ V), due to the less positive potential, with the aim of reducing possible interference (Supplementary data).

4.5. Calibration curve

Fig. 4 depicted CBZ detection at the SiO_2/MWNT/GCE performed by square wave voltammetry (SWV) in 0.1 mol L^{-1} phosphate buffer pH 8.0. The analytical curve (inset Fig. 4) was linear in the concentration range of 0.2 to 4.0 µmol L^{-1}. The linear equation was i_p(A) = $1.39 \times 10^{-6} + 0.485 \times 10^{-6}$ C (mol L^{-1}) with a correlation coefficient of 0.9997. The LOD and quantification limit (LOQ) were found to be 0.056 and 0.187 µmol L^{-1} (S/N = 3), respectively, corresponding to 11 and 36 ppb, which are much lower than the MRLs (100–700 ppb). The LOD and LOQ were calculated by the Miller and Miller statistical method described by da Silva and Machado (2012).

The performance of the SiO_2/MWCNT/GCE was compared to previously reported methods and modified electrodes for the determination of CBZ, as shown in Table 1. We observed that SiO_2/MWCNT/GCE exhibited a low LOD comparable to the previously reported, a wide linear range and the pesticide did not adsorb on the electrode surface, allowing several measurements. Furthermore, the anodic potential was less positive in the pH range studied than those presented by the other modified electrodes, which minimizes interference signals.

4.6. Real sample analysis

To evaluate the proposed analytical method, the SiO_2/MWCNT/GCE was used to detect CBZ in diluted commercial orange juice sample (5.0% (v/v) in 0.1 mol L^{-1} phosphate buffer pH 8.0). No electroanalytical signal which could be explained either by the absence of CBZ or its presence at a concentration below the LOD. Afterwards, the commercial orange juice sample was spiked with CBZ which was determined by SWV (Fig. 5). The voltammograms showed that the current increased linearly with increase of concentration from 0.2 to 3.0 µmol L^{-1} CBZ, according to following equation: i_p (A) = $3.83 \times 10^{-7} + 1.67$ [CBZ] (mol L^{-1}), $r = 0.9927$ (inset Fig. 5). The calculated LOD and LOQ values for the real sample were 0.143 µmol L^{-1} (27 ppb) and 0.476 µmol L^{-1} (91 ppb), respectively. The difference between the LODs and LOQs for spiked water and real sample is probably due to matrix effect or interferences.

4.7. Studies of interference, repeatability, reproducibility and recovery

The influences of some different pesticides in the determination of CBZ were studied. Methomyl and carbaryl pesticides were added (2.0 µmol L^{-1}) to the 0.1 mol L^{-1} phosphate buffer pH 8.0

Table 1
Comparisons among different modified electrodes to assess the CBZ amperometric response.

Method	LOD (mol L^{-1})	Sensitivity (A mol^{-1} L)	Potential (V)	References
Silicone OV-17/GE	4.8×10^{-8} (9.0 ppb)	2.868	Activation step multiple peaks	Hernandez et al. (1996)
MC/GCE	9.6×10^{-7} (184.0 ppb)	0.0896	1.5	Manisankar et al. (2005)
MWNTs/GCE	5.2×10^{-8} (10.0 ppb)	0.1861	1.4	Manisankar, Selvanathan, and Vedhi (2006)
MWNT-PMRE/GCE	9.0×10^{-9} (1.7 ppb)	2.31	1.22	Li and Chi (2009)
CD-GNs/GCE	2.0×10^{-9} (0.4 ppb)	301.02	0.78	Guo et al. (2011)
MWCNT/GCE	5.5×10^{-8} (10.5 ppb)	4.28	0.96	Ribeiro et al. (2011)
GO-MWCNT/GCE	5.0×10^{-9} (1.0 ppb)	2.73	1.1	Luo et al. (2013)
SiO_2/MWCNT/GCE	5.6×10^{-8} (11.0 ppb)	0.485	0.73	Present work

Table 2
Recovery study performed adding standard solutions of CBZ to diluted orange juice samples.

CBZ added ($\mu mol\ L^{-1}$)	Expected value ($\mu mol\ L^{-1}$)	Measured value ($\mu mol\ L^{-1}$)	Recovery (%)	RDS (%)
0.5	0.5	0.47	94.6	0.4
1.0	1.0	1.01	101	1.0
5.0	5.0	5.20	104	1.2

(Supplementary data). No significant electrochemical response was observed in the potential range of CBZ oxidation, either for methomyl or carbaryl, indicating that they do not affect CBZ detection. Besides, the influence of methomyl and carbaryl was verified in the presence of CBZ (2 μM) and no additional electrochemical response or potential shift were observed (Supplementary data). Furthermore, the electrochemical response of ascorbic (AA) and citric acid (CA) were evaluated, because these are the main compounds in orange juice. The addition of ascorbic acid in diluted commercial orange juice sample and in spiked water with 2.0 $\mu mol\ L^{-1}$ CBZ were evaluated (Supplementary data). The results suggest that the proposed sensor was not sensitive to a low ascorbic acid concentration. Higher concentrations of AA (above 50.0 $\mu mol\ L^{-1}$) were detected at potential values quite different from that for CBZ oxidation. The behaviour of ascorbic acid was similar in spiked water and in diluted commercial orange juice. Citric acid did not present any electrochemical signal (Supplementary data). The repeatability of the measurements at the SiO_2/MWCNT/GCE was evaluated by detecting the current response of 2.0 $\mu mol\ L^{-1}$ CBZ at the same modified electrode in 0.1 $mol\ L^{-1}$ phosphate buffer pH 8.0 in the same sample. For five repetitions, the RSD value was 1.4%, which indicated good repeatability of the measurements. The reproducibility of the current responses was measured in spiked water with six different electrodes of the same type and an RSD value of 3.1% was obtained in 0.1 $mol\ L^{-1}$ phosphate buffer pH 8.0 in different samples. These results indicate that the electrode activity and preparation methodology are both suitable for analytical applications.

CBZ recovery data were obtained with the proposed sensor. Standard solutions of CBZ were added to diluted orange juice samples to obtain a final concentration of 0.50 $\mu mol\ L^{-1}$, 1.0 $\mu mol\ L^{-1}$e 5.0 $\mu mol\ L^{-1}$. The recovery (average of three determinations) and precision data are reported in Table 2. The CBZ sensor gave a recovery from 96.4 to 104% and a RSD less than 1.2%.

5. Conclusion

The mesoporous inorganic–organic hybrid material, SiO_2/MWCNT, showed an enhanced electrocatalytic response for CBZ determination with a low LOD. This high electrocatalytic activity is associated with the synergistic association of carbon nanotubes with the silica matrix, with their intimate association revealed by FEG-SEM images and HR-TEM micrographs. This novel material it is possible to detect CBZ in real samples without interference from citric acid, as well as the others carbamate pesticides studied here, and ascorbic acid under 50 μM. Moreover, the hybrid material allowed many sequential analyses with minimal sensor poisoning due to the easy cleaning procedure. These characteristics make this material potentially useful in the development of an electrochemical sensor for carbendazim in real samples.

Acknowledgements

The authors acknowledge the Fundação de Amparo à Pesquisa do Estado de São Paulo (FAPESP) for Grants No. 2011/23047-7 (Thiago C. Canevari), No. 2012/08750-6 (Lívia F. Sgobbi), and No. 2011/10231-4 (Sergio A. S. Machado) and funding from the Coordenação de Aperfeiçoamento de Pessoal de Nível Superior (CAPES).

Appendix A. Supplementary data

Supplementary data associated with this article can be found, in the online version, at http://dx.doi.org/10.1016/j.foodchem.2014.08.085.

References

Backe, W. J., Day, T. C., & Field, J. A. (2013). Zwitterionic, cationic, and anionic fluorinated chemicals in aqueous film forming foam formulations and groundwater from U.S. Military bases by nonaqueous large-volume injection HPLC–MS/MS. *Environmental Science and Technology, 47*(10), 5226–5234.

Buch, A. C., Brown, G. G., Niva, C. C., Sautter, K. D., & Sousa, J. P. (2013). Toxicity of three pesticides commonly used in Brazil to *Pontoscolex corethrurus* (Müller, 1857) and *Eisenia andrei* (Bouché, 1972). *Applied Soil Ecology, 69*, 32–38.

Canevari, T. C., Raymundo-Pereira, P. A., Landers, R., Benvenutti, E. V., & Machado, S. A. S. (2013). Sol–gel thin-film based mesoporous silica and carbon nanotubes for the determination of dopamine, uric acid and paracetamol in urine. *Talanta, 116*, 726–735.

Canevari, T. C., Vinhas, R. C. G., Landers, R., & Gushikem, Y. (2011). $SiO_2/SnO_2/Sb_2O_5$ microporous ceramic material for immobilization of Meldola's blue: Application as an electrochemical sensor for NADH. *Biosensors and Bioelectronics, 26*(5), 2402–2406.

Chiang, Y.-C., Lin, W.-H., & Chang, Y.-C. (2011). The influence of treatment duration on multi-walled carbon nanotubes functionalized by H_2SO_4/HNO_3 oxidation. *Applied Surface Science, 257*(6), 2401–2410.

da Silva, O. B., & Machado, S. A. S. (2012). Evaluation of the detection and quantification limits in electroanalysis using two popular methods: Application in the case study of paraquat determination. *Analytical Methods, 4*(8), 2348–2354.

del Pozo, M., Hernández, L., & Quintana, C. (2010). A selective spectrofluorimetric method for carbendazim determination in oranges involving inclusion-complex formation with cucurbit[7]uril. *Talanta, 81*(4–5), 1542–1546.

Domínguez-Álvarez, J., Mateos-Vivas, M., García-Gómez, D., Rodríguez-Gonzalo, E., & Carabias-Martínez, R. (2013). Capillary electrophoresis coupled to mass spectrometry for the determination of anthelmintic benzimidazoles in eggs using a QuEChERS with preconcentration as sample treatment. *Journal of Chromatography A, 1278*, 166–174.

Ewlad-Ahmed, A. M., Morris, M. A., Patwardhan, S. V., & Gibson, L. T. (2012). Removal of formaldehyde from air using functionalized silica supports. *Environmental Science and Technology, 46*(24), 13354–13360.

Gilbert-López, B., García-Reyes, J. F., & Molina-Díaz, A. (2012). Determination of fungicide residues in baby food by liquid chromatography–ion trap tandem mass spectrometry. *Food Chemistry, 135*(2), 780–786.

Guo, Y., Guo, S., Li, J., Wang, E., & Dong, S. (2011). Cyclodextrin–graphene hybrid nanosheets as enhanced sensing platform for ultrasensitive determination of carbendazim. *Talanta, 84*(1), 60–64.

Hasanzadeh, M., Shadjou, N., Eskandani, M., & de la Guardia, M. (2012). Mesoporous silica-based materials for use in electrochemical enzyme nanobiosensors. *TRAC Trends in Analytical Chemistry, 40*, 106–118.

Hernandez, P., Ballesteros, Y., Galan, F., & Hernandez, L. (1996). Determination of carbendazim with a graphite electrode modified with silicone OV-17. *Electroanalysis, 8*(10), 941–946.

Kundu, S., Wang, Y., Xia, W., & Muhler, M. (2008). Thermal stability and reducibility of oxygen-containing functional groups on multiwalled carbon nanotube surfaces: A quantitative high-resolution XPS and TPD/TPR study. *The Journal of Physical Chemistry C, 112*(43), 16869–16878.

Li, J., & Chi, Y. (2009). Determination of carbendazim with multiwalled carbon nanotubes-polymeric methyl red film modified electrode. *Pesticide Biochemistry and Physiology, 93*(3), 101–104.

Llorent-Martínez, E. J., Fernández-de Córdova, M. L., Ruiz-Medina, A., & Ortega-Barrales, P. (2012). Fluorimetric determination of thiabendazole residues in mushrooms using sequential injection analysis. *Talanta, 96*, 190–194.

Lowell, S., Shields, J. E., Thomas, M., & Thommes, A. M. (2004). *Characterization of porous solids and powders: Surface area, pore size and density*. Boston, USA: Kluwer Academic Publishers.

Luo, S., Wu, Y., & Gou, H. (2013). A voltammetric sensor based on GO-MWNTs hybrid nanomaterial-modified electrode for determination of carbendazim in soil and water samples. *Ionics, 19*(4), 673–680.

Manisankar, P., Selvanathan, G., & Vedhi, C. (2005). Utilization of sodium montmorillonite clay-modified electrode for the determination of isoproturon and carbendazim in soil and water samples. *Applied Clay Science, 29*(3–4), 249–257.

Manisankar, P., Selvanathan, G., & Vedhi, C. (2006). Determination of pesticides using heteropolyacid montmorillonite clay-modified electrode with surfactant. *Talanta, 68*(3), 686–692.

Qu, X., Alvarez, P. J. J., & Li, Q. (2012). Impact of sunlight and humic acid on the deposition kinetics of aqueous fullerene nanoparticles (nC60). *Environmental Science and Technology, 46*(24), 13455–13462.

Ribeiro, W. F., Selva, T. M. G., Lopes, I. C., Coelho, E. C. S., Lemos, S. G., Caxico de Abreu, F., et al. (2011). Electroanalytical determination of carbendazim by square wave adsorptive stripping voltammetry with a multiwalled carbon nanotubes modified electrode. *Analytical Methods, 3*(5), 1202–1206.

Risk assessment for safety of orange juice containing fungicide carbendazim, (2012). Washington DC, USA: U.S. Environmental Protection Agency.

Sing, K. S. W., Everett, D. H., Haul, R. A. W., Moscou, L., Pierotti, R. A., Rouquerol, J., et al. (1985). Reporting physisorption data for gas solid systems with special reference to the determination of surface-area and porosity (Recommendations 1984). *Pure and Applied Chemistry, 57*(4), 603–619.

Subhani, Q., Huang, Z., Zhu, Z., & Zhu, Y. (2013). Simultaneous determination of imidacloprid and carbendazim in water samples by ion chromatography with fluorescence detector and post-column photochemical reactor. *Talanta, 116*, 127–132.

Walcarius, A. (2013). Mesoporous materials and electrochemistry. *Chemical Society Reviews, 42*(9), 4098–4140.

Walcarius, A., Mandler, D., Cox, J. A., Collinson, M., & Lev, O. (2005). Exciting new directions in the intersection of functionalized sol–gel materials with electrochemistry. *Journal of Materials Chemistry, 15*(35–36), 3663–3689.

Wen, Y., Li, J., Yang, F., Zhang, W., Li, W., Liao, C., et al. (2013). Salting-out assisted liquid–liquid extraction with the aid of experimental design for determination of benzimidazole fungicides in high salinity samples by high-performance liquid chromatography. *Talanta, 106*, 119–126.

Yang, W., Ratinac, K. R., Ringer, S. P., Thordarson, P., Gooding, J. J., & Braet, F. (2010). Carbon nanomaterials in biosensors: Should you use nanotubes or graphene? *Angewandte Chemie International Edition, 49*(12), 2114–2138.

Zhou, J.-H., Sui, Z.-J., Zhu, J., Li, P., Chen, D., Dai, Y.-C., et al. (2007). Characterization of surface oxygen complexes on carbon nanofibers by TPD, XPS and FT-IR. *Carbon, 45*(4), 785–796.